

Analysis of Coherence Properties of 3-rd Generation Synchrotron Sources and Free-Electron Lasers

I.A. Vartanyants* and A. Singer

HASYLAB at DESY, Notkestr. 85, D-22607 Hamburg, Germany

Abstract

A general theoretical approach based on the results of statistical optics is used for the analysis of the transverse coherence properties of 3-rd generation synchrotron sources and x-ray free-electron lasers (XFEL). Correlation properties of the wavefields are calculated at different distances from an equivalent Gaussian Schell-model source. This model is used to describe coherence properties of the five meter undulator source at the synchrotron storage ring PETRA III. In the case of XFEL sources the decomposition of the statistical fields into a sum of independently propagating transverse modes is used for the analysis of the coherence properties of these new sources. A detailed calculation is performed for the parameters of the SASE1 undulator at the European XFEL. It is demonstrated that only a few modes contribute significantly to the total radiation field of that source.

PACS numbers: 41.60.Ap, 41.60.Cr, 42.15.Dp, 42.25.Bs, 42.25.Kb

*Corresponding author: Ivan.Vartanyants@desy.de

1 Introduction

With the construction of 3-rd generation, hard x-ray synchrotron sources (ESRF, APS and SPring8) with small source sizes and long distances from source to sample (Fig. 1 (a)), new experiments that exploit the high coherence properties of these x-ray beams have become feasible. New, high brilliance, low emittance, hard x-ray synchrotron sources, such as PETRA III, are under construction [1] and will provide an even higher coherent photon flux for users. Experiments exploiting the coherence properties of these x-ray beams become even more important with the availability of 4-th generation x-ray sources - so-called x-ray free-electron lasers (XFEL) (Fig. 1 (b)). These are presently in the commissioning phase in the USA [2] and under construction in Japan and Europe [3, 4]. Based on the self amplified spontaneous emission (SASE) process [5], they will provide ultrashort, coherent x-ray pulses of unprecedentedly high brightness.

New areas of research have emerged that exploit the high coherence properties of x-ray beams including x-ray photon correlation spectroscopy (XPCS) (for a review see [6, 7]) and coherent x-ray diffractive imaging (CXDI) [8, 9, 10, 11, 12, 13]. In the former, the dynamic properties of a system are studied and in the latter static features are analyzed and a real space image of the sample can be obtained by phase retrieval techniques [14, 15]. Similar ideas can be realized through the use of newly emerging FEL sources. These experiments can be further extended by the use of coherent femtosecond pulses of extremely high intensity. The first demonstration experiments of the possibility of single pulse [16, 17] and single pulse train [18] coherent diffraction imaging were performed recently at the first FEL for extended ultraviolet (XUV) wavelengths, the free-electron laser in Hamburg (FLASH) [19]. In the future, when x-ray FELs with a unique femtosecond time structure will become available, this approach can even be used for different applications in materials science [20], the study of dynamics [21] and biology including such exciting possibilities as single molecule imaging [22].

From these perspectives it is clear that understanding the coherence properties of beams emerging from 3-rd generation synchrotron sources and new FELs is of vital importance for the scientific community. This includes beamline scientists designing beamlines for coherent applications, or experimentalists planning experiments with coherent beams. A beamline scientist, for example, would like to estimate the performance of optics in the partially coherent beam emerging from a synchrotron source. Nowadays, several codes are used for simulation of x-ray propagation from a source through the optical system of a beamline towards an experimental hutch. Most of them are based either on the ray tracing approach (SHADOW [23], RAY [24], *etc.*) which is, in fact, the geometrical optics limit, or on the Fourier optics approach (PHASE [25], *etc.*). It will be shown in our paper that the first approach of ray tracing can be safely used for synchrotron radiation in the horizontal direction, where the radiation field is mostly incoherent, but can not be used in the vertical

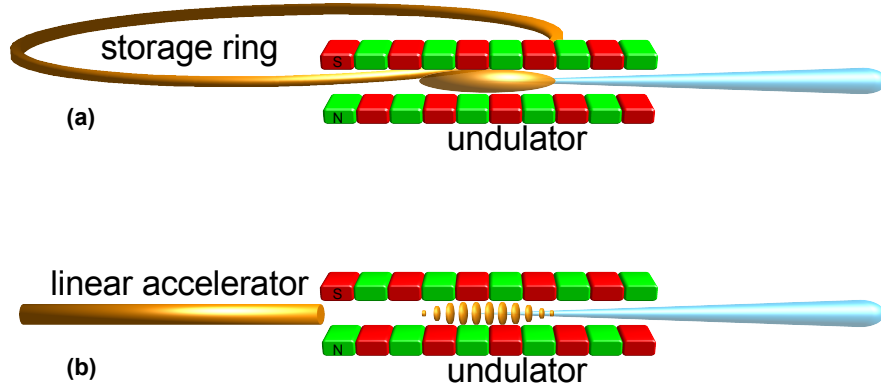


Figure 1: (a) Schematic view of the spontaneous radiation from the undulator source, (b) Schematic view of the coherent radiation from the free-electron laser based on the SASE principle.

direction, where the radiation from the undulator sources is highly coherent. Unfortunately, the approach of Fourier optics in the description of the scattering of synchrotron radiation in the vertical direction is also limited when the radiation is not fully coherent but rather partially coherent. Simulations performed for the XFEL sources at their saturation [26] suggest that these sources are not fully coherent, and as a consequence, partial coherence effects must be carefully considered for them as well. The contribution of partial coherence effects is also important in phase retrieval as a reduced coherence of the incoming beam can produce artifacts in reconstructed images [27, 28, 29].

Different approaches may be used to analyze the coherence properties of the synchrotron and XFEL sources. One is based on a detailed modeling of the radiation process of ultrarelativistic particles in a storage ring or an insertion device (see for e.g. [30, 31]), or a detailed modeling of the SASE process by performing calculations of nonlinear electromagnetic equations at different conditions of operation (linear regime, saturation, etc.) [26]. Another possible approach is based on the results of statistical optics [32, 33], when the statistics of the radiation wavefield is analyzed with the very general assumptions about the origin of the radiators [34, 35, 36]. An attractiveness of this approach is based on the fact that with just a few parameters the coherence properties of the beam can be described at different distances from the source. A famous example of such an approach is the van Cittert-Zernike theorem [32, 33] that predicts the coherence properties of an incoherent source at any distance from that source. The most important assumption when deriving this theorem is that the source is completely incoherent. This means that there are no correlations between any two points of the source at any separation between these two points. As such, it does not require a detailed description of the physical origin of the radiation process of the source. This theorem is

widely applied for the estimate of the coherence properties of 3-rd generation synchrotron sources. This is based on the assumption that each electron in the electron bunch is radiating independently from another electron, which means the radiation should be considered as incoherent. However, this assumption, which is absolutely correct from the point of radiation physics, brings us to a certain contradiction when a radiation field at a large distance from a synchrotron source is analysed. The van Cittert-Zernike theorem gives a realistic estimate of the coherence length downstream from the source, but at the same time it predicts that such a source should radiate in the solid angle of 4π as a completely incoherent source. However, it is well known from electrodynamics (see for e.g. [37]) that ultrarelativistic particles radiate mostly in the forward direction in a narrow cone $\Delta\theta \sim \sqrt{1 - v^2/c^2}$ around the direction of the velocity vector \mathbf{v} , where v is the velocity of the particle and c is the speed of light. As a consequence, typical x-ray beams produced by synchrotron radiation sources have a beam character with a narrow cone and negligible radiation in all other directions. The only way to solve this contradiction in the frame of statistical optics is to assume a certain degree of coherence for a synchrotron source. With this approach we will substitute a real synchrotron source by an *equivalent source* with a certain source size and, what is especially important, a finite degree of coherence that will produce wavefields with the same statistical properties as a radiation field from a real source. With these general assumptions we will use the results of statistical optics to calculate the statistical properties of beams emerging from a new source, PETRA III, at different distances from the source.

We use a different approach for the description of the coherence properties of the FELs. These highly coherent sources can be described with a finite number of transverse modes. We will use a decomposition of the statistical fields into a sum of independently propagating transverse modes and calculate correlation fields at different distances from the source. The source itself will be described by the same Gaussian functions, as in the case of the synchrotron radiation, but clearly with different values of the source parameters. Recently, we characterized the coherence properties of FLASH using this method [38]. For the calculations in this paper we will consider the concrete example of the European XFEL SASE1 undulator source [4]. We will show that for this source only a few modes contribute substantially to the total radiation field.

The paper is organized as follows. In the next section the basic equations of statistical optics will be presented. In section three this general approach will be applied for the characterization of the statistical properties of the beams emerging from the 3-rd generation synchrotron sources. In section four the coherent-mode representation of wavefields will be used for the characterization of the coherence properties of the XFEL beams. The paper ends with the conclusions and an outlook. In the Appendix we compare results obtained in this paper with the theoretical approach developed in Ref. [31] for calculation of coherence properties of radiation emerging from the undulator sources.

2 Basic Equations

2.1 Correlation functions of wavefields

The central concept in the theory of partial coherence is the so-called mutual coherence function (MCF), $\Gamma(\mathbf{r}_1, \mathbf{r}_2; \tau)$, that describes the correlations between two complex scalar¹ values of the electric field at different points \mathbf{r}_1 and \mathbf{r}_2 and at different times. It is defined as [32, 33]

$$\Gamma(\mathbf{r}_1, \mathbf{r}_2; \tau) = \langle E(\mathbf{r}_1, t + \tau) E^*(\mathbf{r}_2, t) \rangle_T, \quad (1)$$

where $E(\mathbf{r}_1, t + \tau)$ and $E(\mathbf{r}_2, t)$ are the field values at the points \mathbf{r}_1 and \mathbf{r}_2 , τ is the time delay, and brackets $\langle \dots \rangle_T$ mean an averaging over times T much longer than the fluctuation time of the x-ray field. It is also assumed that the radiation is ergodic and stationary. From the definition of the MCF it follows that when two points coincide an averaged intensity is given by

$$\langle I(\mathbf{r}) \rangle = \Gamma(\mathbf{r}, \mathbf{r}; 0) = \langle E(\mathbf{r}, t) E^*(\mathbf{r}, t) \rangle_T. \quad (2)$$

It is usual to normalize the MCF as

$$\gamma(\mathbf{r}_1, \mathbf{r}_2; \tau) = \frac{\Gamma(\mathbf{r}_1, \mathbf{r}_2; \tau)}{\sqrt{\langle I(\mathbf{r}_1) \rangle} \sqrt{\langle I(\mathbf{r}_2) \rangle}}, \quad (3)$$

which is known as the complex degree of coherence. For all values of the arguments $\mathbf{r}_1, \mathbf{r}_2$ and τ the absolute value of the complex degree of coherence $0 \leq |\gamma(\mathbf{r}_1, \mathbf{r}_2; \tau)| \leq 1$.

Following Mandel & Wolf [33] the cross-spectral density (CSD) function, $W(\mathbf{r}_1, \mathbf{r}_2, \omega)$, can be introduced. According to its definition it forms a Fourier transform pair with the MCF in the time-frequency domain

$$W(\mathbf{r}_1, \mathbf{r}_2; \omega) = \int_{-\infty}^{\infty} \Gamma(\mathbf{r}_1, \mathbf{r}_2; \tau) e^{i\omega\tau} d\tau. \quad (4)$$

The cross-spectral density is a measure of correlation between the spectral amplitudes of any particular frequency component ω of the light vibrations at the points \mathbf{r}_1 and \mathbf{r}_2 . When two points \mathbf{r}_1 and \mathbf{r}_2 coincide, the CSD represents the spectral density, $S(\mathbf{r}, \omega)$, (or the power spectrum) of the field

$$S(\mathbf{r}, \omega) = W(\mathbf{r}, \mathbf{r}; \omega). \quad (5)$$

Introducing the normalized cross-spectral density function, $\mu(\mathbf{r}_1, \mathbf{r}_2; \omega)$, which is called the spectral degree of coherence (SDC) at frequency ω , we obtain

$$\mu(\mathbf{r}_1, \mathbf{r}_2; \omega) = \frac{W(\mathbf{r}_1, \mathbf{r}_2; \omega)}{\sqrt{S(\mathbf{r}_1, \omega)} \sqrt{S(\mathbf{r}_2, \omega)}}, \quad (6)$$

¹In the following, for simplicity, we consider only one polarization of the x-ray field.

where again, as for the case of the complex degree of coherence, the following inequality is valid $0 \leq |\mu(\mathbf{r}_1, \mathbf{r}_2; \omega)| \leq 1$.

In order to characterize the transverse coherence properties of the wavefields by one number the degree of the transverse coherence can be introduced as [26]

$$\zeta(\omega) = \frac{\int |\mu(\mathbf{r}_1, \mathbf{r}_2; \omega)|^2 S(\mathbf{r}_1; \omega) S(\mathbf{r}_2; \omega) d\mathbf{r}_1 d\mathbf{r}_2}{\left| \int S(\mathbf{r}; \omega) d\mathbf{r} \right|^2}. \quad (7)$$

According to its definition the values of the parameter $\zeta(\omega)$ lie in the range $0 \leq \zeta(\omega) \leq 1$.

For narrow bandwidth light the complex degree of coherence can be approximated by $\gamma(\mathbf{r}_1, \mathbf{r}_2; \tau) \approx \gamma(\mathbf{r}_1, \mathbf{r}_2; 0) \exp(-i\bar{\omega}\tau)$ leading to a relationship $|\gamma(\mathbf{r}_1, \mathbf{r}_2; \tau)| = |\mu(\mathbf{r}_1, \mathbf{r}_2; \bar{\omega})|$, where $\bar{\omega}$ is the average frequency. In the same conditions, similar relationships can be obtained for the spectral density and the average intensity $S(\mathbf{r}, \omega) = \langle I(\mathbf{r}) \rangle \delta(\omega - \bar{\omega})$, where $\delta(\omega)$ is the delta function. As a consequence, for narrow bandwidth light, the spectral density is equivalent to the average intensity.

2.2 Coherent-mode representation of correlation functions

It has been shown [33], that under very general conditions, one can represent the CSD of a partially coherent, statistically stationary field of any state of coherence as a sum of independent coherent modes

$$W(\mathbf{r}_1, \mathbf{r}_2; \omega) = \sum_j \beta_j(\omega) E_j^*(\mathbf{r}_1; \omega) E_j(\mathbf{r}_2; \omega), \quad (8)$$

where $\beta_j(\omega)$ and $E_j(\mathbf{r}; \omega)$ are the eigenvalues and eigenfunctions, that satisfy the Fredholm integral equation of the second kind

$$\int W(\mathbf{r}_1, \mathbf{r}_2; \omega) E_j(\mathbf{r}_1; \omega) d\mathbf{r}_1 = \beta_j(\omega) E_j(\mathbf{r}_2; \omega). \quad (9)$$

The eigenfunctions in (8-9) form an orthogonal set.

According to the definition of the spectral density, $S(\mathbf{r}, \omega)$, (5) we have in the case of a coherent-mode representation of the fields

$$S(\mathbf{r}, \omega) = \sum_j \beta_j(\omega) |E_j(\mathbf{r}; \omega)|^2. \quad (10)$$

2.3 Propagation of the wavefield correlation functions in the free space

For our purposes it is especially important to calculate correlation functions at different distances from the source. Propagation of the cross-spectral density

$W(\mathbf{r}_1, \mathbf{r}_2; \omega)$ in the half space $z > 0$ from the source plane at $z = 0$ to the plane at distance z in paraxial approximation is determined by the following expression [33]

$$W(\mathbf{r}_1, \mathbf{r}_2, z; \omega) = \int_{\Sigma} \int_{\Sigma} W_S(\mathbf{s}_1, \mathbf{s}_2, 0; \omega) P_z^*(\mathbf{r}_1 - \mathbf{s}_1; \omega) P_z(\mathbf{r}_2 - \mathbf{s}_2; \omega) d\mathbf{s}_1 d\mathbf{s}_2, \quad (11)$$

where $W_S(\mathbf{s}_1, \mathbf{s}_2, 0; \omega)$ is the value of the CSD at the source plane $z = 0$, $P_z(\mathbf{r} - \mathbf{s}; \omega)$ is the Green function (or propagator), and the integration is made in the source plane. In Eq. (11) and below coordinates \mathbf{s}_1 and \mathbf{s}_2 are taken in the plane of the source and coordinates \mathbf{r}_1 and \mathbf{r}_2 are taken in the plane at the distance z . The propagator $P_z(\mathbf{r} - \mathbf{s}; \omega)$ describes the propagation of radiation in free space and is defined as

$$P_z(\mathbf{r} - \mathbf{s}; \omega) = \frac{1}{i\lambda z} \exp \left[i \frac{k}{2z} (\mathbf{r} - \mathbf{s})^2 \right], \quad (12)$$

where $k = 2\pi/\lambda$ and λ is the wavelength of radiation.

In the case of the coherent-mode representation of the correlation functions, the values of the CSD can be obtained at different distances by propagating the individual coherent modes. Propagation of the individual modes in the half space $z > 0$ from the source plane at $z = 0$ to the plane at distance z in the paraxial approximation can be obtained from

$$E_j(\mathbf{r}, z; \omega) = \int_{\Sigma} E_j^S(\mathbf{s}; \omega) P_z(\mathbf{r} - \mathbf{s}; \omega) d\mathbf{s}, \quad (13)$$

where $E_j^S(\mathbf{s}; \omega)$ are the values of the field amplitudes at the source plane, $z = 0$, and $P_z(\mathbf{r} - \mathbf{s}; \omega)$ is the same propagator as in (12). Due to the statistical independence of the modes [33], the CSD, after propagating a distance z , is given as a sum of propagated modes $E_j(\mathbf{r}, z; \omega)$ with the same eigenvalues $\beta_j(\omega)$ defined as in (9)

$$W(\mathbf{r}_1, \mathbf{r}_2, z; \omega) = \sum_j \beta_j(\omega) E_j^*(\mathbf{r}_1, z; \omega) E_j(\mathbf{r}_2, z; \omega). \quad (14)$$

3 Coherence properties of 3-rd generation synchrotron sources

3.1 Gaussian Schell-model source

In this section we apply the general theory of the propagation of Gaussian optical beams from a source of any state of coherence to the case of synchrotron radiation. We assume that a *real* synchrotron source (for example an insertion device like an undulator) can be represented by its *equivalent* model

that produces x-ray radiation with statistical properties similar to a real x-ray source. This equivalent model source will be positioned in the center of the real undulator source.

We will assume that the x-ray radiation is generated by a planar Gaussian Schell-model (GSM) source [39]. Such sources are described by the following CSD function [33]

$$W_S(\mathbf{s}_1, \mathbf{s}_2) = \sqrt{S_S(\mathbf{s}_1)}\sqrt{S_S(\mathbf{s}_2)}\mu_S(\mathbf{s}_2 - \mathbf{s}_1), \quad (15)$$

where the spectral density and SDC of the x-ray beam in the source plane are Gaussian functions²

$$\begin{aligned} S_S(\mathbf{s}) &= S_{0x}S_{0y} \exp\left(-\frac{s_x^2}{2\sigma_{Sx}^2} - \frac{s_y^2}{2\sigma_{Sy}^2}\right), \\ \mu_S(\mathbf{s}_2 - \mathbf{s}_1) &= \exp\left(-\frac{(s_{2x} - s_{1x})^2}{2\xi_{Sx}^2} - \frac{(s_{2y} - s_{1y})^2}{2\xi_{Sy}^2}\right). \end{aligned} \quad (16)$$

Here parameters $\sigma_{Sx,y}$ define the rms source size in the x - and y - directions and $\xi_{Sx,y}$ give the coherence length of the source in the respective directions.

The starting expression for the source cross-spectral density function in the form of expression (15), is in fact, very general and is based on the definition of the SDC (6). Here, the main approximations are that the source is modeled as a plane two-dimensional source, that the spectral density, $S_S(\mathbf{s})$, and the SDC, $\mu_S(\mathbf{s}_2 - \mathbf{s}_1)$, (16) are Gaussian functions, and that the source is spatially uniform (SDC $\mu_S(\mathbf{s}_2 - \mathbf{s}_1)$ depends only on the difference of spatial coordinates \mathbf{s}_1 and \mathbf{s}_2). The fact that synchrotron radiation sources are typically elongated in the horizontal direction is specifically introduced in the expression (16) by allowing the source size $\sigma_{Sx,y}$ and coherence length of the source $\xi_{Sx,y}$ to be different in x - and y - direction. What is especially important in this model is the assumption of a certain degree of coherence of the source expressed by a finite coherence length of that source $\xi_{Sx,y}$. Only with this finite coherence length of the source it is possible to get a reasonable description of the synchrotron radiation with its extremely small divergence.

It can be shown [33], that with a suitable choice of source size, σ_S , and coherence length, ξ_S , a GSM source can generate a field whose intensity has appreciable values only within a narrow cone of solid angle. In optics radiation with a narrow angular divergence is called a beam. This will be a good model for x-ray beams generated by insertion devices, such as undulators, which produce x-ray beams with a divergence of a few micro radians. In order to generate the beam, the parameters of a GSM source have to satisfy the following inequality in each direction

$$\frac{1}{\delta_{Sx,y}^2} \ll \frac{2\pi^2}{\lambda^2}, \quad (17)$$

²In this equation and below the frequency dependence ω is omitted.

where

$$\frac{1}{\delta_{Sx,y}^2} = \frac{1}{(2\sigma_{Sx,y})^2} + \frac{1}{\xi_{Sx,y}^2}. \quad (18)$$

For x-ray wavelengths of about 0.1 nm we get for the right hand side of this inequality $2 \cdot 10^9 \text{ } 1/\mu\text{m}^2$. The smallest size of a source that is at the moment available at 3-rd generation synchrotron in the vertical direction is of the order of a few microns. We have not yet estimated the coherence length ξ_S of the source, but as we will see later it is also of the order of a few microns. From these estimates, it is seen that the beam condition (17) is very well satisfied for x-ray wavelengths and 3-rd generation synchrotron sources. This gives us confidence using the beam approach to describe the properties of the x-ray radiation from these sources.

There are two important limits which we can describe as an incoherent or coherent source. The source will be called *incoherent* if its coherence length ξ_S is much smaller than the source size $\xi_S \ll \sigma_S$. From the beam condition (17) we find for this source

$$\delta_S \approx \xi_S \gg \frac{1}{\sqrt{2\pi}} \lambda.$$

This means that to satisfy the beam conditions for a spatially incoherent source the coherence length has to be small but at the same time larger than the wavelength $\sigma_S \gg \xi_S \gg \lambda$. In the opposite limit of a spatially *coherent* source $\xi_S \gg \sigma_S$ we find from the beam condition (17)

$$\delta_S \approx 2\sigma_S \gg \frac{1}{\sqrt{2\pi}} \lambda.$$

This means that to satisfy the beam condition for a spatially coherent source the source size should be larger than the wavelength $\xi_S \gg \sigma_S \gg \lambda$.

Integration in (11) with the CSD $W_S(\mathbf{s}_1, \mathbf{s}_2)$ (15, 16) can be done independently for each dimension. This gives the following expression for the CSD $W(x_1, x_2, z)^3$ at distance z from the source [40, 41] (see also Mandel & Wolf [33])

$$W(x_1, x_2, z) = \frac{I_{0x}}{\Delta_x(z)} e^{i\psi_x(z)} \exp \left[-\frac{(x_1 + x_2)^2}{8\sigma_{Sx}^2 \Delta_x^2(z)} \right] \exp \left[-\frac{(x_2 - x_1)^2}{2\delta_{Sx}^2 \Delta_x^2(z)} \right]. \quad (19)$$

Here

$$\Delta_x(z) = \left[1 + \left(\frac{z}{z_x^{eff}} \right)^2 \right]^{1/2} \quad (20)$$

is called an expansion coefficient and

$$\psi_x(z) = \frac{k(x_2^2 - x_1^2)}{2R_x(z)}, R_x(z) = z \left[1 + \left(\frac{z_x^{eff}}{z} \right)^2 \right] \quad (21)$$

³Below we present results only in x -direction. The same equations are valid in y -direction.

are the phase and the radius of curvature of a Gaussian beam. In Eqs. (20, 21) an effective distance z_x^{eff} is introduced that is defined as

$$z_x^{eff} = k\sigma_{Sx}\delta_{Sx}. \quad (22)$$

At that distance the expansion coefficient $\Delta(z_x^{eff}) = \sqrt{2}$. In the limit of a spatially coherent source $\delta_S \approx 2\sigma_S$ and an effective distance z_x^{eff} coincides with the so-called Rayleigh length $z_R = 2k\sigma_{Sx}^2$, which is often introduced in the theory of optical Gaussian beams [42]. According to Eq. (20) an effective distance z_x^{eff} can serve as a measure of the distances, where nonlinear effects in the propagation of the beams are still strong. Distances $z \gg z_x^{eff}$ can be considered as a far-field limit where the expansion parameter $\Delta_x(z) \rightarrow z/z_x^{eff}$ and the radius $R_x(z) \rightarrow z$ change linearly with the distance z .

Setting $x_1 = x_2 = x$ in Eq. (19) we obtain for the spectral density

$$S(x, z) = \frac{I_{0x}}{\Delta_x(z)} \exp \left[-\frac{x^2}{2\Sigma_x^2(z)} \right], \quad (23)$$

where

$$\Sigma_x(z) = \sigma_{Sx}\Delta_x(z) = [\sigma_{Sx}^2 + \theta_{\Sigma x}^2 z^2]^{1/2} \quad (24)$$

is an rms size of the x-ray beam at a distance z from the source. In Eq. (24) $\theta_{\Sigma x}$ is the angular divergence of the beam

$$\theta_{\Sigma x} = \frac{1}{2k\xi_{Sx}} [4 + q_{Sx}^2]^{1/2}. \quad (25)$$

Here a ratio of the coherence length to the source size

$$q_{Sx} = \frac{\xi_{Sx}}{\sigma_{Sx}} \quad (26)$$

is introduced. It can be considered as a measure of the degree of coherence of the source.

According to its definition (6) and (19, 23), the spectral degree of coherence at a distance z from the source is given by

$$\mu(x_1, x_2, z) = e^{i\psi_x(z)} \exp \left[-\frac{(x_2 - x_1)^2}{2\Xi_x^2(z)} \right], \quad (27)$$

where

$$\Xi_x(z) = \xi_{Sx}\Delta_x(z) = [\xi_{Sx}^2 + \theta_{\Xi x}^2 z^2]^{1/2} \quad (28)$$

is the effective coherence length of an x-ray beam at the same distance. In Eq. (28) $\theta_{\Xi x}$ is the angular width of the coherent part of the beam

$$\theta_{\Xi x} = \frac{1}{2k\sigma_{Sx}} [4 + q_{Sx}^2]^{1/2}. \quad (29)$$

For the *incoherent* source ($q_{Sx} \ll 1$) we have from (25, 29)

$$\theta_{\Sigma x} = \frac{1}{k\xi_{Sx}}, \theta_{\Xi x} = \frac{1}{k\sigma_{Sx}}. \quad (30)$$

It is seen immediately that in this limit equation (28) predicts the same values for the coherence length $\Xi_x(z)$ at large distances z as given by the van Zittert-Cernike theorem. At the same time expression (30) gives an estimate for the divergence of the beam from an incoherent source, which is determined by the coherence length ξ_{Sx} of the source. So, directly from (30), we have an estimate of the coherence length of the incoherent source

$$\xi_{Sx} = \frac{\lambda}{2\pi\theta_{\Sigma x}}. \quad (31)$$

In another limit of a *coherent* source, when parameter $q_{Sx} \gg 1$, we obtain from (25, 29)

$$\theta_{\Sigma x} = \frac{1}{2k\sigma_{Sx}}, \theta_{\Xi x} = \frac{1}{2k\sigma_{Sx}}q_{Sx}. \quad (32)$$

In this coherent limit the angular width of the coherent part of the beam exceeds the angular divergence of the beam, which is determined now only by the size of the source, and we are approaching here the limit of a so-called diffraction limited source.

In the frame of the GSM, the coherence length of the source of any state of coherence can be expressed conveniently through its emittance $\varepsilon_{Sx} = \sigma_{Sx}\sigma'_{Sx}$, where σ'_{Sx} is the rms of the angular divergence of the source. It can be obtained by inverting the full expression of the angular divergence of the beam (25)

$$\xi_{Sx} = \frac{2\sigma_{Sx}}{\sqrt{4k^2\varepsilon_{Sx}^2 - 1}} \quad (33)$$

and the substitution of the angular divergence $\theta_{\Sigma x}$ by σ'_{Sx} .

One important property of the beams generated by the GSM sources is that at any distance from the source the ratio of the coherence length $\Xi_x(z)$ to the beam size $\Sigma_x(z)$ is a constant value and is equal to the same ratio at the source. From Eqs. (24, 28) we have for the parameter q_x

$$q_x = \frac{\xi_{Sx}}{\sigma_{Sx}} = \frac{\Xi_x(z)}{\Sigma_x(z)}. \quad (34)$$

The degree of transverse coherence ζ_x introduced in Eq. (7) can be directly calculated for the GSM source and related to the values of q_x by the following expression

$$\zeta_x = \frac{q_x}{\sqrt{q_x^2 + 4}}. \quad (35)$$

According to the relationship (34) the values of the degree of transverse coherence ζ_x for the GSM are preserved for any distance z from the source.

Table 1: Parameters of the high brilliance synchrotron radiation source PETRA III for a 5 m undulator [1] (energy $E=12$ keV, distance from the source $z=60$ m)

	High-β		Low-β	
	x	y	x	y
Source size σ_S , [μm]	141	5.5	36	6
Source divergence σ'_S , [μrad]	7.7	3.8	28	3.7
Transverse coherence length at the source ξ_S , [μm]	2.07	4.53	0.57	4.65
Degree of coherence q	0.015	0.82	0.016	0.77
Degree of transverse coherence ζ	0.008	0.38	0.008	0.36
Effective length z^{eff} , [m]	18.33	1.48	1.29	1.63
Beam size at distance z $\Sigma(z)$, [mm]	0.48	0.23	1.68	0.22
Transverse coherence length at distance z $\Xi(z)$, [μm]	7.08	187.8	26.5	170.5

The emittance of a GSM source ε_{Sx} can be expressed through the degree of the transverse coherence ζ_x . From Eqs. (25) and (35) we have for the emittance of a GSM source

$$\varepsilon_{Sx} = \frac{1}{2k\zeta_x}. \quad (36)$$

Taking into account that for a source of any degree of coherence the values of ζ_x lie in the range $0 \leq \zeta_x \leq 1$ the values of the emittance should satisfy an inequality $\varepsilon_{Sx} \geq 1/2k = \lambda/4\pi$. For a fully coherent source $\zeta_x \rightarrow 1$ and the emittance $\varepsilon_{Sx}^{coh} = \lambda/4\pi$. This value can be considered as the emittance of a diffraction limited source. For an incoherent source $\zeta_x \rightarrow 0$ and according to Eq. (36) $\varepsilon_{Sx} \gg \lambda/4\pi$.

3.2 Transverse coherence properties of the PETRA III source

Our previous analysis can be effectively used to estimate the coherence properties of the beams produced by 3-rd generation x-ray sources if source parameters (source size and divergence) are known. We will make this calculation for the high brilliance synchrotron source PETRA III that is presently under construction at DESY. This storage ring is planned to produce $\varepsilon_x = 1$ nm emittance beams in the horizontal direction and, due to 1% coupling, the emittance in the vertical direction will be two orders of magnitude lower.

Source parameters for a 5 m long undulator and a photon energy of 12 keV are summarized in Table 1. Two cases of high- β and low- β operation are considered. The values of the coherence length of the source calculated according to Eq. (33) vary from 0.6 to 2 microns in the horizontal direction and are about 5 microns in the vertical. We can estimate the values of the parameter

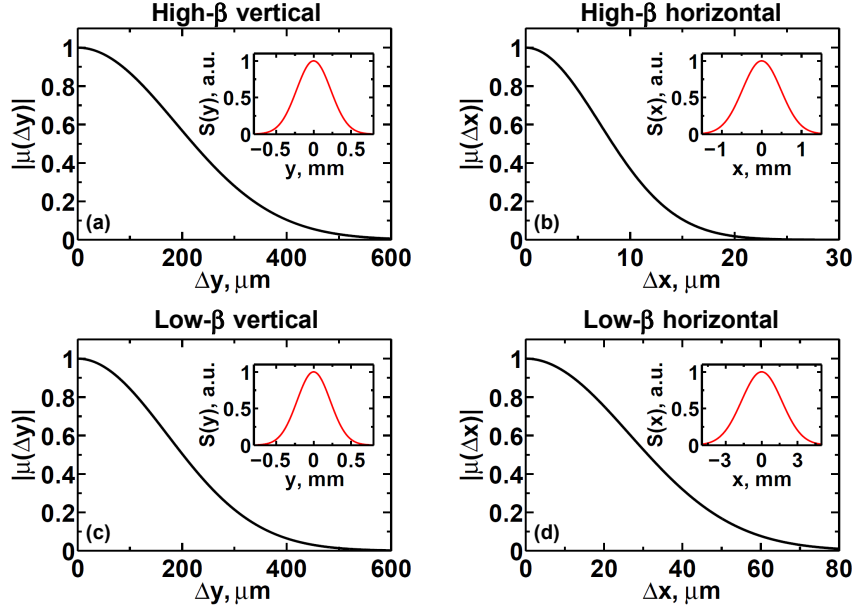


Figure 2: The absolute value of the spectral degree of coherence $|\mu(\Delta x)|$ as a function of separation of two points across the beam at a distance of 60 m downstream from the source. The spectral density $S(x)$ as a function of the position across the beam calculated at the same distance from the source is shown in the insets. The rms values of the beam size $\Sigma_{x,y}(z)$ and transverse coherence length $\Xi_{x,y}(z)$ at that distance were taken from Table 1. (a, b) High- β vertical and horizontal sections of the beam. (c, d) Low- β vertical and horizontal sections of the beam.

q_S (34) and the degree of transverse coherence ζ_S of that source. Using tabulated values of the source size we get for the horizontal direction $q_{Sx} \sim 0.02$ and for the vertical $q_{Sy} \sim 0.8$. For the degree of transverse coherence ζ_S (35) we have in the horizontal direction $\zeta_{Sx} \sim 0.01$ and in the vertical $\zeta_{Sy} \sim 0.4$. These estimates immediately show that in the horizontal direction PETRA III source is a rather incoherent source with the degree of coherence about 1%, however in the vertical direction the coherence length of the source is about the size of the source itself, and it can be considered as a rather coherent source with a degree of coherence about 40%. Substituting these numbers into (24, 28) we can obtain the values of the intensity distribution and the transverse coherence length at any distance downstream from the source. These values are listed in Table 1 for a distance $z = 60 \text{ m}$, where the first experimental hutches are planned. We see that for this distance the coherence length is varying from $7 \mu\text{m}$ to $25 \mu\text{m}$ in the horizontal direction and is in the range from $170 \mu\text{m}$ to $190 \mu\text{m}$ in the vertical one. This defines the coherence area across the beam within which one can plan experiments with coherent beams.

The absolute value of the SDC, $|\mu(\Delta x)|$, (27) as a function of the separation

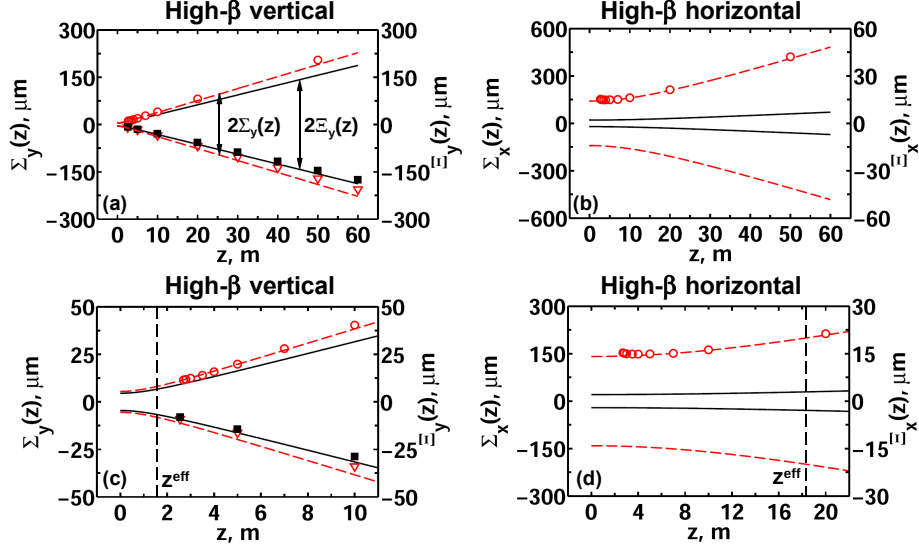


Figure 3: The beam size $\Sigma_{x,y}(z)$ and the transverse coherence length $\Xi_{x,y}(z)$ at different distances z from the source for a high- β section of the PETRA III storage ring. Parameters of the source are taken from Table 1. In all figures the dashed (red) line is the beam size $\Sigma_{x,y}(z)$ and the solid (black) line is the transverse coherence length $\Xi_{x,y}(z)$. Open circles correspond to calculations performed by the ESRF simulation code SRW [43], open triangles are the beam size and squares are the transverse coherence length obtained from the analytical results of Ref. [31]. (a, c) Vertical direction of the beam. (b, d) Horizontal direction of the beam. The vertical dashed line in (c) and (d) correspond to an effective distance z^{eff} . Note, different range for the coherence length comparing to that of the beam size in (b,d).

of two points across the beam and the spectral density, $S(x)$, (23) as a function of the position across the beam at a distance 60 m downstream from the source are presented in Fig. 2. The rms values of the beam size $\Sigma_{x,y}(z)$ and transverse coherence length $\Xi_{x,y}(z)$ were taken from Table 1. It can be seen in Figs. 2 (a,c) that the properties of the beam in the vertical direction are very similar for both the high- β and low- β operation of the PETRA III source. The FWHM of the beam is about 500 μm in both cases. For separations of up to 100 μm the beam is highly coherent (with the degree of coherence higher than 80%). In the horizontal direction (Figs. 2 (b,d)) the situation is quite different. The FWHM of the beam for high- β operation is about one millimeter and for low- β operation the beam is quite divergent and its FWHM is about three millimeters. It is well seen in Figs. 2 (b,d) that the beam is rather incoherent in the horizontal direction. The degree of coherence is higher than 80% for separations of up to 15 μm for a low- β operation and 5 μm for a high- β operation at this distance.

Calculations of the beam size, $\Sigma_{x,y}(z)$, and the transverse coherence length, $\Xi_{x,y}(z)$, at different distances z from the source are made according to Eqs. (24, 28). They are presented for high- β operation in Fig. 3 and for low- β operation

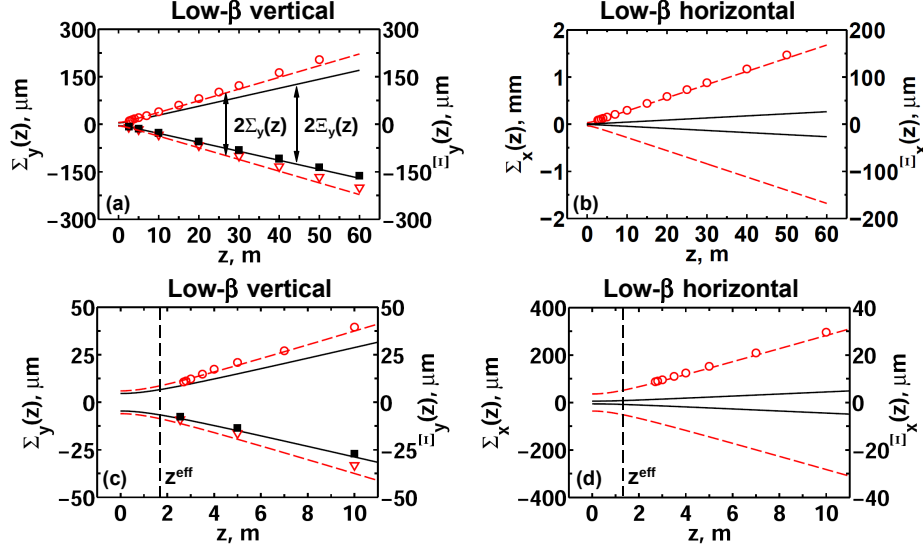


Figure 4: The same as in Fig. 3 for a low- β section of the PETRA III storage ring.

in Fig. 4. These calculations show that in the vertical direction the properties of the beam along the beamline for both high- β and low- β operations of the PETRA III source are quite similar. The rms values of the coherence length, $\Xi_{x,y}(z)$, (black, solid line) are slightly smaller than the rms values of the beam size, $\Sigma_{x,y}(z)$, (red, dash line) along the beamline. At distances larger than $z_y^{eff} \simeq 1.5$ m in the vertical direction all z -dependencies can be considered to be linear. It means that for all practical cases all parameters scale linearly with the distance z . In the horizontal direction the situation is quite different. Firstly as expected and clearly seen in Figs. 3 and 4, the beam is quite incoherent in this direction. It is also three times more divergent in the far-field for low- β operation (Fig. 4 (b)). It is interesting to note that the linear z -dependence of parameters $\Sigma_x(z)$ and $\Xi_x(z)$ for high- β operation starts from further distances from the source. An effective distance z_y^{eff} is about 20 m in this case.

We compared the results obtained by our approach with the results of different calculations performed for the PETRA III five meter undulator source by the ESRF simulation code SRW [43] as well as by the analytical results obtained in Ref. [31] (see Appendix for details). Our calculations show that the divergence of the beam both in the vertical and in the horizontal directions is well described by our model as compared with the SRW calculations (see Fig. 3 and Fig. 4). The comparison with the results of Ref. [31] was performed only in the vertical direction as in the horizontal direction the source can be described as a quasi-homogeneous source (coherence length of such a source is much smaller than the size of the source ($\xi_{Sx} \ll \sigma_{Sx}$)). In this limit the analytical results of Ref. [31] completely coincide with our description of the source in the frame of the GSM. However, in the vertical direction a more

careful analysis is required. Using the approach of Ref. [31] we calculated the SDC and spectral density for a five meter undulator of the PETRA III source in the vertical direction at different distances z from the source. From these calculations we obtained the rms values of the source size $\Sigma_x(z)$ and the coherence length $\Xi_x(z)$ at different distances from the source and compared them with the results obtained from the GSM (see Figs. 3 (a,c) and Figs 4 (a,c)). This comparison shows very good agreement between two approaches for these energies. However, the analytical approach of Ref. [31] gives slightly lower values of the beam size and the coherence length at larger distances. The lower values of the beam size predicted by Ref. [31] can be attributed to effects of a final energy spread of electrons in the bunch that were neglected in calculations. From this comparison, we see that an approach based on the GSM and simulations performed by different methods at a wavelength of 0.1 nm give similar results⁴.

4 Coherence properties of x-ray free-electron lasers

4.1 Coherent-mode decomposition for the GSM source

We apply a general approach of coherent-mode decomposition, described in section two, for the analysis of the correlation properties of wavefields originating from XFEL sources. We substitute a real XFEL source by an equivalent planar GSM source (15, 16). Coherent modes and eigenvalues obtained as a solution of the Fredholm integral equation (9) for such a GSM source are well known [44, 45] and can be decomposed for each transverse direction $E_{l,m}(s_x, s_y) = E_l(s_x)E_m(s_y)$ and $\beta_{l,m} = \beta_l\beta_m$. The eigenvalues β_j for the GSM source have a power law dependence and the eigenfunctions $E_j(s_x)$ at such a source are described by the Gaussian Hermite-modes⁵ [46]

$$\beta_j/\beta_0 = \kappa^j, \quad (37)$$

$$E_j(s_x) = \frac{k^{1/4}}{(\pi z_x^{eff})^{1/4}} \frac{1}{(2^j j!)^{1/2}} H_j \left(\sqrt{\frac{k}{z_x^{eff}}} s_x \right) \exp \left[- \left(\frac{k}{2z_x^{eff}} \right) s_x^2 \right], \quad (38)$$

where $H_j(x)$ are the Hermite polynomials of order j , $\beta_0 = \sqrt{8\pi} S_{0x} \sigma_{Sx} \delta_{Sx} / (2\sigma_{Sx} + \delta_{Sx})$, and $\kappa = (2\sigma_{Sx} - \delta_{Sx}) / (2\sigma_{Sx} + \delta_{Sx})$. The parameters σ_{Sx} , δ_{Sx} and z_x^{eff} have the same meaning as in Eqs. (16, 18, 22).

Equation (37) for the eigenvalues of the GSM source gives, in fact, the relative weights with which the different modes contribute to the CSD of the

⁴We performed a similar analysis for different energies and came to the conclusion that for PETRA III source parameters the GSM model can be safely used at energies higher than 6 keV (see Appendix for details).

⁵Due to the symmetry of the Gaussian-Schell model we consider below only one transverse direction.

source. It can be also expressed through the values of the parameter q_x (34) [33], or through the values of the degree of transverse coherence ζ_x (35)

$$\frac{\beta_j}{\beta_0} = \left[\frac{1}{(q_x^2/2) + 1 + q_x [(q_x/2)^2 + 1]^{1/2}} \right]^j = \left(\frac{1 - \zeta_x}{1 + \zeta_x} \right)^j. \quad (39)$$

For a spatially coherent source ($\xi_{Sx} \gg \sigma_{Sx}$) we have from Eq. (39)

$$\frac{\beta_j}{\beta_0} \approx q_x^{-2j}. \quad (40)$$

According to this equation $\beta_j \ll \beta_0$ for all $j \neq 0$ that means that in the coherent limit the source can be well characterized by its lowest mode. In the opposite limit of an incoherent source ($\xi_{Sx} \ll \sigma_{Sx}$) we have from Eq. (39)

$$\frac{\beta_j}{\beta_0} \approx 1 - jq_x. \quad (41)$$

According to this equation many modes are necessary for a sufficient description of the source.

Correlation properties of the fields in the coordinate-frequency domain at any distance z from the source can be calculated with the help of expression (14) by propagating individual modes $E_j(x, z)$. In the case of the GSM source the propagated modes $E_j(x, z)$ at a distance z from the source are described by the following expression [46]

$$\begin{aligned} E_j(x, z) = & \frac{k^{1/4}}{\left(\pi z_x^{eff} \Delta_x^2(z) \right)^{1/4}} \frac{1}{(2^j j!)^{1/2}} H_j \left[\sqrt{\frac{k}{z_x^{eff}}} \left(\frac{x}{\Delta_x(z)} \right) \right] \times \\ & \times \exp \left[-\frac{k}{2z_x^{eff}} \left(\frac{x}{\Delta_x(z)} \right)^2 \right] \times \\ & \times \exp \left\{ i[kz - (j+1)\phi_x(z)] + \frac{ikx^2}{2R_x(z)} \right\}, \end{aligned} \quad (42)$$

where $\phi_x(z) = \arctan(z/z_x^{eff})$. Parameters $\Delta_x(z)$ and $R_x(z)$ have the same meaning as in (20, 21). For $j = 0$ these modes coincide with an expression for a monochromatic Gaussian beam propagating from a Gaussian source.

4.2 Transverse coherence properties of the European XFEL source

We used this approach to make a realistic and simple estimate of the coherence properties of the upcoming XFEL sources. For detailed calculations we took parameters of the SASE1 undulator at the European XFEL reported in [4] (see also Ref. [26]) and summarized in Table 2. Simulations were made for a

Table 2: Parameters of the SASE1 undulator of the European XFEL [4]

	SASE1 undulator
Wavelength λ , [nm]	0.1
Source size σ_S , [μm]	29.7
Source divergence σ'_S , [μrad]	0.43
Transverse coherence length at the source ξ_S , [μm]	48.3
Degree of coherence q	1.63
Degree of transverse coherence ζ	0.63
Effective length z^{eff} , [m]	70

GSM source (15, 16) with an rms source size $\sigma_S = 29.7 \mu\text{m}$ and a transverse coherence length at the source of $\xi_S = 48.3 \mu\text{m}$. The latter parameter was obtained from Eq. (33) using the values of the source size and angular divergence listed in Table 2. With these parameters the CSD, $W(x_1, x_2; z)$, (14) was calculated at a distance of 500 m from the source with the eigenvalues β_j and eigenfunctions $E_j(x, z)$ evaluated from Eqs. (37, 42). A distance of 500 m was considered because at this distance the first optical elements of the European XFEL are planned. In Fig. 5 the results of these calculations are presented. An analysis of the results shows that for the parameters of the SASE1 undulator at XFEL a small number of transverse modes contribute to the total field (Fig. 5 (c)). Parameter $\kappa = 0.22$ in these conditions, which means that the contribution of the first mode is about 20% of the fundamental and the contribution of the fourth mode is below one per cent of the fundamental $\beta_4/\beta_0 = \kappa^4 = 2.3 \times 10^{-3}$. Finally, five modes (including the fundamental) were used in (14) for calculations of the CSD $W(x_1, x_2; z)$ (Fig. 5 (a)). From the obtained values of the CSD, the modulus of the SDC, $|\mu(x_1, x_2, z)|$, (Figs. 5 (b,d)) and the spectral density, $S(x)$, at that distance were evaluated. As our source is described as a Gaussian source these functions are Gaussian as well. At a distance $z = 500$ m from the source we obtained a coherence length $\Xi(z) = 348 \mu\text{m}$ and a beam size $\Sigma(z) = 214 \mu\text{m}$.

Analysis of Fig. 5 (d) shows that our model source, though being highly coherent, can not be described as a fully coherent source. The problem lies in the contribution of the higher modes to the fundamental. This is illustrated in more detail in Fig. 6 where the spectral degree of coherence, $|\mu(\Delta x)|$, is calculated with a different number of contributing modes at separation distances of up to 1 mm where the spectral density $S(x)$ is significant. It is readily seen from this figure that only in the case of a single mode contribution will an XFEL beam be fully coherent (Fig. 6 (a)). As soon as the first transverse mode contributes to the fundamental, the SDC, $|\mu(\Delta x)|$, drops quickly and reaches zero at a separation distance of $\Delta x \approx 700 \mu\text{m}$ (Fig. 6 (b)). It again in-

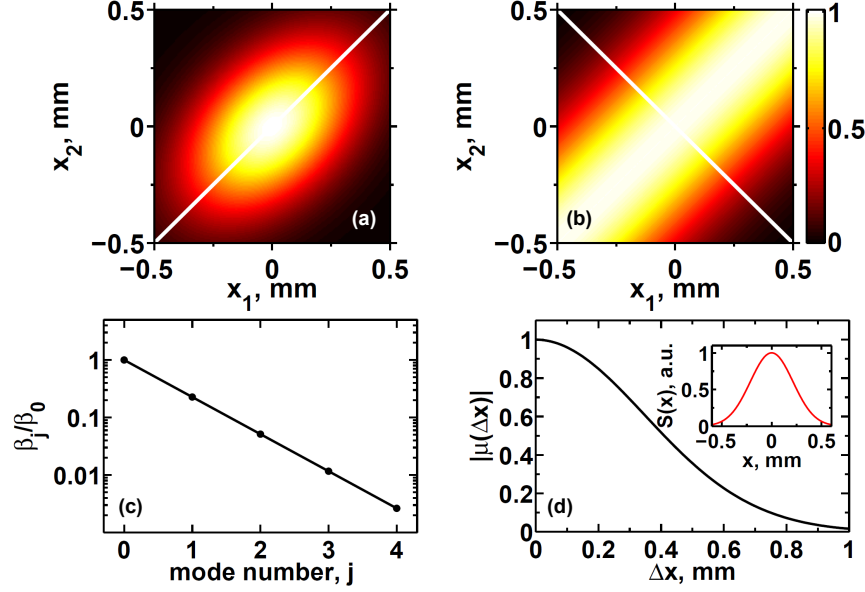


Figure 5: Calculations of the coherence properties of the SASE1 undulator at the European XFEL (see Table 2) 500 m downstream from the source in the frame of a GSM source. (a) The absolute value of the cross-spectral density $|W(x_1, x_2)|$. (b) The absolute value of the spectral degree of coherence $|\mu(x_1, x_2)|$. (c) The ratio β_j/β_0 of the eigenvalue β_j to the lowest order eigenvalue β_0 as a function of mode number j . (d) The absolute value of the spectral degree of transverse coherence $|\mu(\Delta x)|$ taken along the white line in (b). In the inset spectral density $S(x)$ is shown that is taken along the white line in (a).

creases up for higher separation distances and reaches the value $|\mu(\Delta x)| = 0.3$ at $\Delta x \approx 1$ mm. This increase in the correlation function is due to the fact that at these distances the contribution of the lowest mode (fundamental in this particular case) is negligible and the correlation properties are determined again by a single mode (the first in this case). This effect is demonstrated in Fig. 7, where the contribution of different modes to the spectral density is presented. In this particular case the spectral density can be well described by three modes.

The values of the beam size $\Sigma(z)$ and the transverse coherence length $\Xi(z)$ at different distances z from our GSM source are presented in Fig. 8. Calculations were performed using a coherent-mode decomposition (14) of the CSD $W(x_1, x_2; z)$ at different distances from the GSM source. It can be seen from Fig. 8 that contrary to the analysis performed for a synchrotron source, here, in the case of the European XFEL, the values of the transverse coherence length $\Xi(z)$ are higher than the values of the beam size $\Sigma(z)$ at all distances from the source downstream. An effective distance z^{eff} (22) is about 70 m in this case, which means that for distances $z \gg 70$ m all z -dependencies of

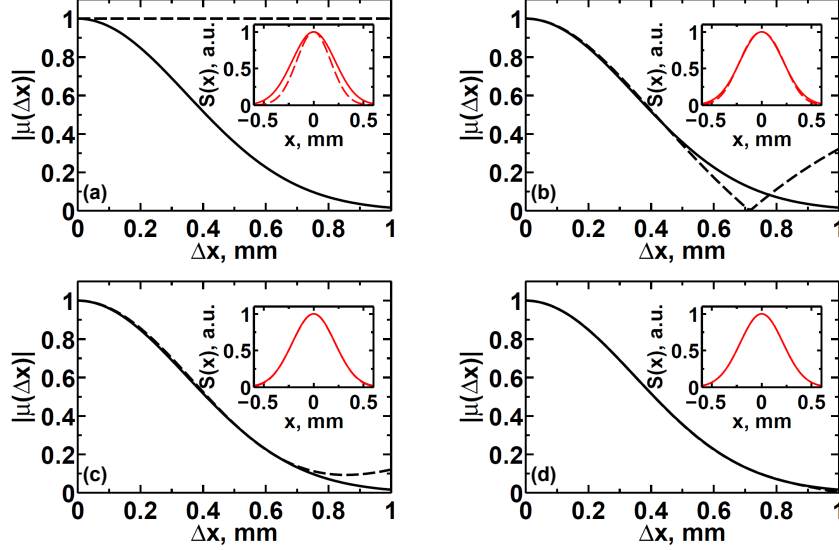


Figure 6: Contribution of the higher transverse modes to the absolute value of the spectral degree of coherence $|\mu(\Delta x)|$. The same for the spectral density $S(x)$ is shown in the insets. (a) Fundamental mode contribution, (b) fundamental plus first mode contribution, (c) fundamental plus two modes contribution, (d) fundamental plus three modes contribution. In all figures the dashed line corresponds to an actual number of modes contributing to $|\mu(\Delta x)|$ and $S(x)$. In all figures solid line corresponds to a full calculation of $|\mu(\Delta x)|$ and $S(x)$ with the five modes. Calculations were made for the same parameters as in Fig. 5.

parameters, such as the coherence length and the beam size, can be considered to be linear.

Using the previously introduced values of the degree of the transverse coherence ζ (35) and the parameters obtained for an equivalent GSM source (see Table 2) we find that $\zeta = 0.63$ for that source. This means we can expect a transverse coherence of about 60% at the European XFEL. This number is in good agreement with the value $\zeta = 0.65$ obtained by the ensemble average of the wavefields produced by the SASE1 undulator of the European XFEL calculated by the code FAST using the actual number of electrons in the beam [26]. This good agreement obtained for the value of the degree of the transverse coherence ζ by different approaches gives good fidelity for the analysis proposed in this work based on the results of statistical optics and a simple characterization of the source with a GSM.

Here, for a sufficient description of the transverse coherence properties of FELs, we used a coherent-mode decomposition approach. In principle, the same approach can be used for the description of the 3-rd generation synchrotron sources, however being mostly incoherent sources, especially in the horizontal direction, they would require a large number of modes for a sufficient description. This is illustrated in Fig. 9 where the ratio β_j/β_0 of the

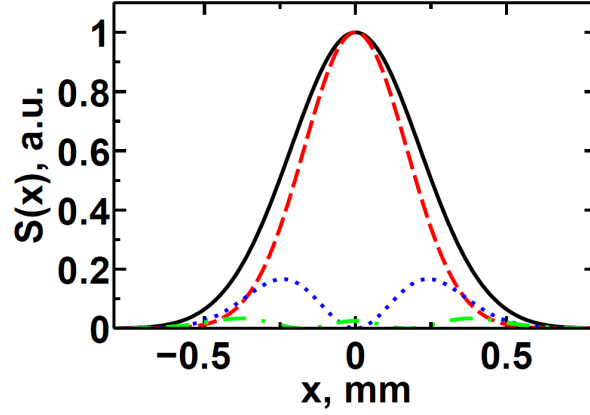


Figure 7: Contribution of the higher transverse modes to the spectral density $S(x)$. The solid (black) line corresponds to a full calculation of $S(x)$ with the five modes. The dashed (red) line is the fundamental mode contribution. The dotted (blue) line is the first mode contribution and dash dotted (green) line is the second mode contribution. Calculations were made for the same parameters as in Fig. 5.

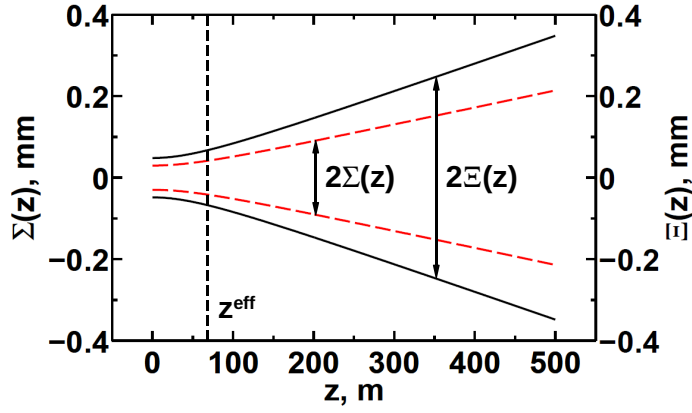


Figure 8: The beam size $\Sigma(z)$ (dashed line) and the transverse coherence length $\Xi(z)$ (solid line) at different distances z from the SASE1 undulator of the European XFEL source. Parameters of the source are the same as in Fig. 5. The vertical dashed line correspond to an effective distance z^{eff} .

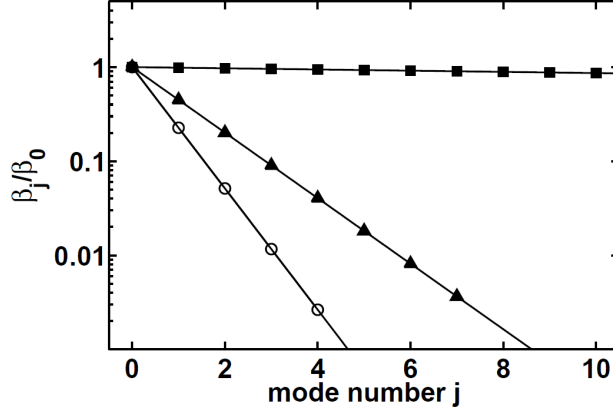


Figure 9: The ratio β_j/β_0 of the eigenvalue β_j to the lowest order eigenvalue β_0 as a function of mode number j . Results of the calculations for the parameters of the SASE1 undulator of the European XFEL (open circles), high- β section of the five meter undulator of the PETRA III source in the vertical direction (triangles) and in the horizontal direction (squares).

eigenvalue β_j to the lowest order eigenvalue β_0 as a function of a mode number j for the PETRA III synchrotron source is presented. For comparison, results of the calculations for the SASE1 undulator of the European XFEL are also shown in the same figure. In the calculations we considered the same PETRA III parameters as in the previous section (see Table 1, high- β operation of the PETRA III storage ring). Our results demonstrate that in the vertical direction correlation functions can be properly described by the contribution of eight modes (including the fundamental) and in the horizontal direction a large number of modes (about 300) is necessary to describe the coherence properties of the undulator source. This is in good agreement with the behavior of the modes described by Eqs. (40, 41) for a coherent and an incoherent source. Our results indicate that in the vertical direction the undulator source is highly coherent, however in the horizontal direction it behaves as an incoherent source.

5 Summary

In summary, we have demonstrated how a general theoretical approach based on the results of statistical optics can be applied to give a sufficient description of the correlation properties of the fields generated by 3-rd generation synchrotron sources and FELs. We have substituted a real source by an equivalent planar GSM source with the same source size and divergence as a real source. This phenomenological approach gives us the opportunity to characterize this source with just two parameters, source size and transverse coherence length. What is more important is that this approach can be used as a tool to calculate correlation functions at different distances from the source

with simple analytic functions. In this way, realistic estimates of the size of an x-ray beam and its coherence length can be obtained at any distance from the source. This also gives a beam profile and a complex degree of coherence in the transverse direction at any distance from the source.

We applied this general approach to the concrete case of the PETRA III source that is under construction. Our calculations have shown that the coherence properties of this synchrotron source are quite different in the vertical and the horizontal directions (this is typical of all 3-rd generation synchrotron sources). In the vertical direction a beam produced with the parameters of PETRA III is highly coherent with a degree of coherence of about 40%, however, in the horizontal direction it is a rather incoherent source with a degree of coherence of about 1%. Sixty meters downstream from that source, where the first experimental hutches are planned, the transverse coherence length in the vertical direction reaches a value of $190\text{ }\mu\text{m}$ and in the horizontal direction can be about $25\text{ }\mu\text{m}$. This has to be compared with the size of the beam at the same distance with the FWHM values about 0.5 mm in the vertical and 1 mm in the horizontal directions. The values of the transverse coherence length and the beam size scale linearly at these large distances from the source and can be easily estimated at any other distance from the source.

In the case of the XFELs we used a decomposition of the statistical fields into a sum of independently propagating transverse modes for the analysis of the coherence properties of these fields at different distances from the source. Calculations were performed for the concrete case of the SASE1 undulator at the European XFEL, which is presently under construction. Our analysis has shown that only a few transverse modes (five in the case of European XFEL) contribute significantly to the total radiation field of the XFEL. It was demonstrated that due to the contribution of a few transverse modes, the SASE1 undulator source while being highly coherent (with the degree of coherence about 60%), can not be considered as fully coherent. One essential difference between the radiation field from the XFEL compared with that of a synchrotron source is that its coherence properties are expected to be of the same order of magnitude in the vertical as well as in the horizontal direction (compare with the results of the measurements performed at FLASH [38]). The transverse coherence length 500 m downstream from the source, where the first optical elements will be located, is expected to be of the order of $350\text{ }\mu\text{m}$ compared to the FWHM of the beam that is expected to be about $500\text{ }\mu\text{m}$.

The approach used in this paper for the analysis of the transverse coherence properties is quite general and can be applied as an effective and useful tool for describing the coherence properties of undulator radiation at 3-rd generation synchrotron sources and of SASE FELs. In our future work, we plan to extend this approach to calculate the coherence properties of x-ray beams passing through different optical elements.

Appendix

We compared results obtained by the GSM with the results of Ref. [31] for the PETRA III synchrotron source and different photon energies ranging from 3 keV to 20 keV (see Figs. A1, A2). There are two critical dimensionless parameters of the theory [31]

$$D_{x,y} = k\sigma'_{x,y}L_u \text{ and } N_{x,y} = \frac{k\sigma_{x,y}^2}{L_u}, \quad (\text{A-1})$$

where $\sigma_{x,y}$ and $\sigma'_{x,y}$ are the electron bunch sizes and divergences in the horizontal and in the vertical directions and L_u is the undulator length. The electron beam sizes $\sigma_{x,y}$ and divergences $\sigma'_{x,y}$ can be calculated from the values of the emittance $\varepsilon_{x,y}$ and known β -function of the synchrotron source according to $\sigma_{x,y} = \sqrt{\varepsilon_{x,y}\beta_{x,y}}$, $\sigma'_{x,y} = \sqrt{\varepsilon_{x,y}/\beta_{x,y}}$ (see e.g. [35]). As it was shown in Ref. [31], for large parameter values $D_{x,y} \gg 1$ and $N_{x,y} \gg 1$ the undulator source can be described in the frame of the GSM (see Eqs. (15, 16)) with the source size $\sigma_{Sx,y} = \sqrt{N_{x,y}L_u/k}$ and parameter $\delta_{Sx,y}$ (18) $\delta_{Sx,y} = \sqrt{L_u/kD_{x,y}}$. Using the values of $D_{x,y}$ and $N_{x,y}$ (A-1) and the definition of $\delta_{Sx,y}$ (18) we obtain for the source size $\sigma_{Sx,y} = \sigma_{x,y}$ and the coherence length $\xi_{Sx,y}$ at the source $\xi_{Sx,y} = 2\sigma_{x,y}/\sqrt{4k^2\varepsilon_{x,y}^2 - 1}$. These expressions are exactly the same as discussed earlier in the paper (compare for e.g. Eq. (33) for the coherence length $\xi_{Sx,y}$) with the only exception that here the electron beam parameters are used instead of the photon beam parameters. For the PETRA III parameters at the photon energy of $E = 12$ keV and low- β operation (see Table 1 and PETRA III TDR [1]) we obtain $D_x = 234$, $D_y = 1.0$ and $N_x = 16$, $N_y = 0.36$. We can see from these estimates that in the horizontal direction parameters $D_x \gg 1$, $N_x \gg 1$ that means that in this direction GSM can be safely used. However, in the vertical direction at the same energy $D_y \leq 1$, $N_y \leq 1$, and a more careful analysis has to be applied.

To compare predictions of the GSM theory with the theoretical results of Ref. [31] in the vertical direction we used the far-field expressions for the cross-spectral density function $W(\bar{y}, \Delta y)$ (Eq. (65) from Ref. [31]) and spectral density $S(y)$ (Eq. (71) from Ref. [31]) obtained in the limit $D_x \gg 1$ and $N_x \gg 1$. The SDC $\mu(\bar{y}, \Delta y)$ was calculated according to Eq. (6)

$$\mu(\bar{y}, \Delta y) = \frac{W(\bar{y}, \Delta y)}{\sqrt{S(\bar{y} + \Delta y/2)}\sqrt{S(\bar{y} - \Delta y/2)}}, \quad (\text{A-2})$$

where $\bar{y} = (y_1 + y_2)/2$, $\Delta y = y_2 - y_1$ and y_1 , y_2 are two positions in the vertical direction. Calculations were performed for a five meter undulator of the PETRA III source, high- β and low- β operation, 60 m downstream from the source at the central position of the beam ($\bar{y} = 0$). In Figs. A1 and A2 results of the calculations of the SDC and spectral density for the energy range from 3 keV up to 20 keV are presented (see for the parameters used in these simulations Tables A1 and A2). These results are compared with the GSM

High- β operation

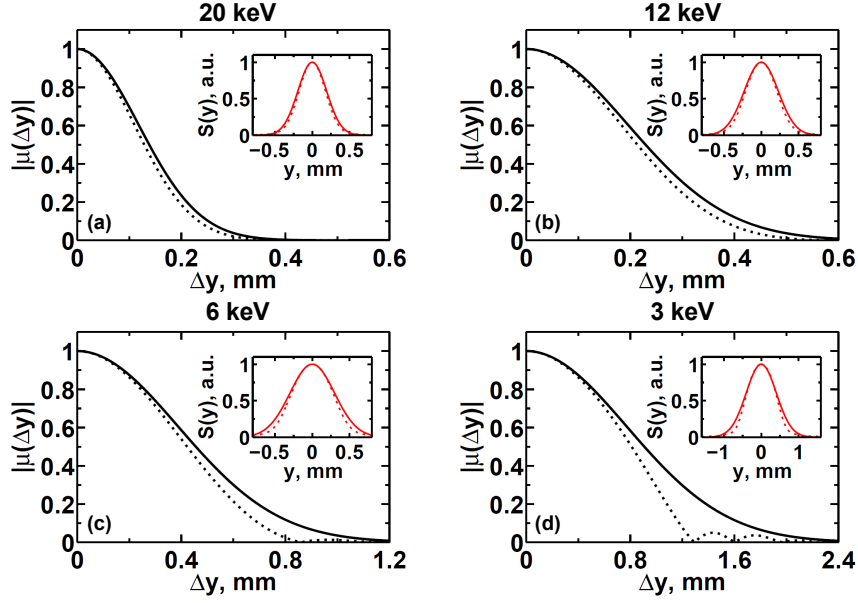


Figure A1: The absolute value of the spectral degree of coherence $|\mu(\Delta y)|$ in the vertical direction at the distance 60 m downstream from the source for a high- β operation calculated for different photon energies ((a) 20 keV, (b) 12 keV, (c) 6 keV, (d) 3 keV) using results of Ref. [31] (dotted line). The spectral density $S(y)$ (dotted line) calculated in the same conditions is shown in the insets. For comparison, calculations performed in the frame of the GSM are also shown in this figure (solid lines).

theory described in this paper. For the GSM calculations at different photon energies the total photon source size σ_{Ty} and divergence σ'_{Ty} were used. They are determined from a convolution of the sizes and divergences of the electron beam (σ_y, σ'_y) with the intrinsic radiation characteristics of a single electron (σ_r, σ'_r). The latter are given by [35] $\sigma_r = \sqrt{2\lambda L_u}/4\pi, \sigma'_r = \sqrt{\lambda/2L_u}$.

As we can see from Figs. A1 and A2, in spite of the fact that parameters $D_y \leq 1, N_y \leq 1$ (see Tables A1 and A2), the difference between two approaches is negligible down to an energy of 6 keV. It becomes more pronounced only at energies of about 3 keV for large separation distances Δy . It is also interesting to note that the coherence area, defined as the area where the degree of coherence drops to 80%, is the same in both approaches down to a lowest energy of 3 keV. At the same time, for this very low energy the effects of the single electron radiation (at the photon energy $E = 3$ keV $\sigma_r \geq \sigma_y$ and $\sigma'_r \geq \sigma'_y$) are becoming more pronounced and reveal themselves in the form of oscillations at large separations Δy . An inspection of Figs. A1 and A2 shows that the GSM slightly overestimates the values of the SDC compared to the results of Ref. [31]. We relate this to the fact that at low energies, at the source position, the intensity distribution obtained in the frame of the model

Low- β operation

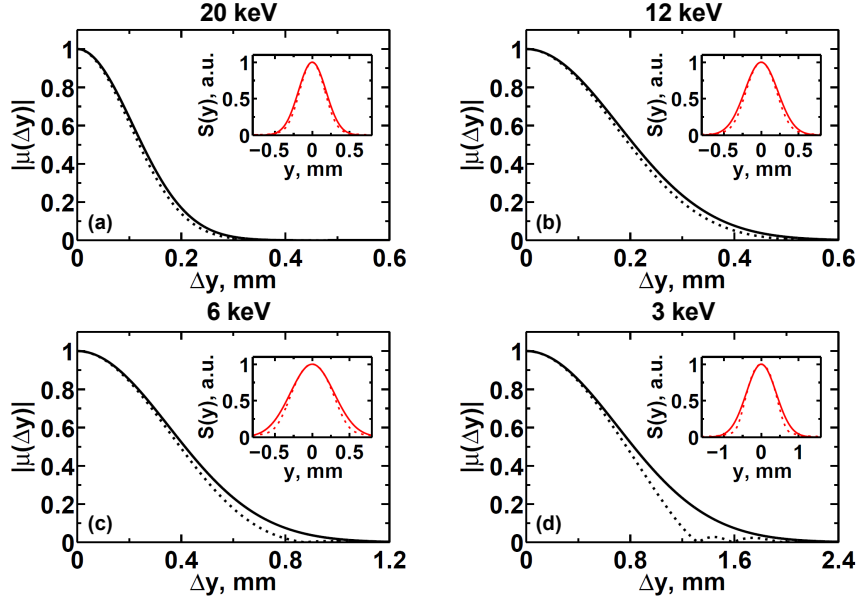


Figure A2: The same as in Fig. A1 for a low- β section of the PETRA III storage ring.

[31] contains long tails that effectively produce a larger source size in comparison to a source size obtained by the GSM approach. We note here as well that according to the Tables A1 and A2 the approximation $D_x \gg 1$ and $N_x \gg 1$ is no longer valid at very low energies below 3 keV. Consequently, at these low energies Eqs. (65, 71) from Ref. [31] can not be applied for calculation of the coherence properties of the five meter undulator source at PETRA III. A more careful treatment using general expressions for the correlation functions should be used in this case.

In conclusion, our analysis shows that for the high brilliance source PETRA III the GSM can be safely used for the five meter undulator at x-ray energies higher than 6 keV. It will also give a reasonable upper limit estimate of the coherence length for the energies as low as 3 keV. Our analysis has also shown that for a shorter undulator of 2 m length, which is typical for the PETRA III source, both approaches give similar results even for lower energies.

Acknowledgments

We acknowledge the help of M. Tischer in calculation of the radiation properties of the 5 m PETRA III undulator using SRW code and the interest and support of E. Weckert during the work on this project. We also acknowledge a fruitful discussion with E. Saldin and M. Yurkov and careful reading of the manuscript by A. Mancuso.

Table A1: Parameters of the synchrotron radiation source PETRA III for a 5 m undulator, high- β operation, and different photon energies. Parameters $N_{x,y}$, $D_{x,y}$ are defined in Eq. (A-1), $\sigma_{Tx,y}$ and $\sigma'_{Tx,y}$ are the total photon source sizes and divergences, σ_r and σ'_r are the intrinsic radiation characteristics of a single electron. The following electron beam sizes $\sigma_x = 141 \mu\text{m}$, $\sigma_y = 4.9 \mu\text{m}$ and divergences $\sigma'_x = 7.1 \mu\text{rad}$, $\sigma'_y = 2.0 \mu\text{rad}$ were used in these calculations.

	20 keV	12 keV	6 keV	3 keV
N_x	405	243	122	61
D_x	25	15	7.6	3.8
N_y	0.5	0.30	0.15	0.07
D_y	2.0	1.3	0.63	0.32
$\sigma_{Tx}, \mu\text{m}$	141	141	141	142
$\sigma'_{Tx}, \mu\text{rad}$	7.5	7.7	8.4	9.6
$\sigma_{Ty}, \mu\text{m}$	5.3	5.5	6.1	7.1
$\sigma'_{Ty}, \mu\text{rad}$	3.2	3.8	5.0	6.7
$\sigma_r, \mu\text{m}$	2.0	2.6	3.6	5.1
$\sigma'_r, \mu\text{rad}$	2.5	3.2	4.5	6.4

Table A2: The same as in Table A1 for the low- β operation of the synchrotron source. The following electron beam sizes $\sigma_x = 36 \mu\text{m}$, $\sigma_y = 5.5 \mu\text{m}$ and divergences $\sigma'_x = 28 \mu\text{rad}$, $\sigma'_y = 1.8 \mu\text{rad}$ were used here, σ_r and σ'_r are the same as in Table A1.

	20 keV	12 keV	6 keV	3 keV
N_x	26	16	7.9	4.0
D_x	390	234	117	58
N_y	0.61	0.36	0.18	0.09
D_y	1.7	1.0	0.51	0.25
$\sigma_{Tx}, \mu\text{m}$	36	36	36	36
$\sigma'_{Tx}, \mu\text{rad}$	28	28	28	28
$\sigma_{Ty}, \mu\text{m}$	5.8	6.0	6.6	7.5
$\sigma'_{Ty}, \mu\text{rad}$	3.1	3.7	4.9	6.7

References

- [1] PETRA III: A Low Emittance Synchrotron Radiation Source. Technical Design Report. (Ed. K. Balewski, W. Brefeld, W. Decking, H. Franz, R. Röhlsberger, E. Weckert. DESY, Hamburg, Germany. February 29, 2004).
- [2] J. Arthur *et al*, Linac Coherent Light Source (LCLS) Conceptual Design Report, SLAC-R-593, April 2002,
<http://www.slac.stanford.edu/pubs/slacreports/slac-r-593.html>.
See also: P. Emma, *et al*, <http://www-ssrl.slac.stanford.edu/lcls/commissioning/documents/th3pbi01.pdf>
- [3] T. Tanaka, T. Shintake, Eds, SCSS X-FEL Conceptual Design Report, SCSS XFEL, RIKEN, Japan, 2005, RIKENHarimaInstitute/SPRING-8, 1-1-1, Kouto, Mikazuki, Sayo, HyogoJAPAN 679-5148, <http://www-xfel.spring8.or.jp/>.
- [4] M. Altarelli, *et al.*, (Eds.), XFEL The European X-ray Free-Electron Laser. Technical Design Report, DESY 2006-097 (2006), http://xfel.desy.de/tdr/index_eng.html.
- [5] E.L. Saldin, E.A. Schneidmiller, and M.V. Yurkov, *The Physics of Free Electron Lasers* (Springer-Verlag, Berlin, 2000).
- [6] G. Grübel and F. Zontone, J. Alloys and Compounds **362**, 3 (2004).
- [7] F. Livet, Acta Cryst **A63**, 87 (2007).
- [8] J. Miao, P. Charalambous, J. Kirz and D. Sayre, Nature **400**, 342 (1999).
- [9] M. Pfeifer, G. Williams, I. Vartanyants, R. Harder, and I. K. Robinson, Nature **442**, 63 (2006).
- [10] H.N. Chapman, A. Barty, S. Marchesini, *et al.*, J. Opt. Soc. Am. A **23**, 1179 (2006).
- [11] D. Shapiro, P. Thibault, T. Beetz, *et al.*, PNAS **102**, 15343-15346, (2005).
- [12] B. Abbey, K. A. Nugent, G. J. Williams, *et al.*, Nature Physics **4**, 394 (2008).
- [13] P. Thibault, M. Dierolf, A. Menzel, *et al.*, Science **321**, 379 (2008).
- [14] J. R. Fienup, Appl. Opt. **21**, 2758 (1982).
- [15] V. Elser, J. Opt. Soc. Am. A **20**, 40 (2003).
- [16] H.N. Chapman, A. Barty, M.J. Bogan, *et al.*, Nature Physics **2**, 839 (2006).

- [17] H. N. Chapman, S. P. Hau-Riege, M. J. Bogan, *et al.*, Nature **448**, 676 (2007).
- [18] A.P. Mancuso, A. Schropp, B. Reime, *et al.*, Phys. Rev. Lett. **102**, 035502/1-5 (2009).
- [19] W. Ackermann *et al.*, Nature Photonics, **1**, 336 (2007).
- [20] I.A. Vartanyants, I. K. Robinson, I. McNulty, *et al.*, J. Synchrotron Rad. **14**, 453–470 (2007).
- [21] G. Grübel, G.B. Stephenson, C. Gutt, *et al.*, Nucl. Instrum. Methods B **262**, 357 (2007).
- [22] R. Neutze, R. Wouts, D. van der Spoel, E. Weckert, and J. Hajdu Nature **406**, 752 (2000).
- [23] For code SHADOW see: http://www.nanotech.wisc.edu/CNT_LABS/shadow.html.
- [24] For code RAY see: F. Schäfers, BESSY Tech. Ber. **202/96**, 1 (1996).
- [25] For code PHASE see: http://www.helmholtz-berlin.de/forschung/gross-geraete/undulatoren/arbeitsgebiete/phase_en.html.
- [26] E.L. Saldin, E.A. Schneidmiller, M.V. Yurkov, Optics Commun. **281**, 1179 (2008).
- [27] I.A. Vartanyants and I.K. Robinson, J.Phys.: Condens. Matter **13**, 10593 (2001).
- [28] I.A. Vartanyants and I.K. Robinson, Optics Commun. **222** 29 (2003).
- [29] G.J. Williams, H.M. Quiney, A.G. Peele, and K.A. Nugent, Phys. Rev. B **75**, 104102 (2007).
- [30] Y. Takayama, T. Hatano, T. Miyakava, and W. Okamoto, J. Synchrotron Rad. **5** 1187-1194 (1998).
- [31] G. Geloni, E. Saldin, E. Schneidmiller, M. Yurkov, NIM in Physics Research A 588 463-493 (2008).
- [32] J. W. Goodman, Statistical Optics, Wiley, New York, 1985.
- [33] L. Mandel and E. Wolf, Optical Coherence and Quantum Optics, Cambridge University Press, Cambridge, 1995.
- [34] K.-J. Kim, Nucl. Instr. and Meth. A **246**, 71 (1986); K.-J. Kim, SPIE Proc. **582**, 2 (1986).

- [35] M.R. Howells and M.M. Kincaid, The properties of undulator radiation, in *New Directions in Research with Third-generation Soft X-Ray Synchrotron Radiation Sources*, Kluwer Academic Publishers, Dordrecht, 1994, pp. 315-358.
- [36] R. Coisson, Applied Optics **34**(5), 904 (1995); R. Coisson and S. Marchesini, J. Synchrotron Rad. **4**, 263 (1997).
- [37] L.D. Landau and E.M. Lifshits, The Classical Theory of Fields, Forth Edition Vol. 2 (Course of Theoretical Physics Series) (Butterworth-Heinemann, Oxford, 1980).
- [38] A. Singer, I.A. Vartanyants, M. Kuhlmann, *et al.*, Phys. Rev. Lett. **101**, 254801 (2008).
- [39] The applicability of the Gaussian Schell-model for the description of the synchrotron radiation is discussed in details in Refs. [30, 31, 35, 36].
- [40] A.T. Friberg and R.J. Sudol, Opt. Commun. (1982) **41**, 383.
- [41] A.T. Friberg and R.J. Sudol, Opt. Acta (1983) **30**, 1075.
- [42] A.E. Siegman, *An Introduction to Lasers and Masers* (McGraw-Hill, New York, 1971).
- [43] O. Chubar, P. Elleaume, SRW, Version 3.7 ESRF 1997-2000 <http://www.esrf.eu/Accelerators/Groups/InsertionDevices/Software/SRW>.
- [44] F. Gori, Opt. Commun. **34**, 301 (1980).
- [45] A. Starikov and E. Wolf, J. Opt. Soc. Am. **72** 923 (1982).
- [46] F. Gori, Opt. Commun. **46**, 149 (1983).